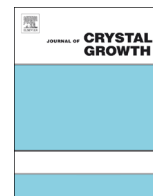




ELSEVIER

Contents lists available at ScienceDirect

Journal of Crystal Growth

journal homepage: www.elsevier.com/locate/jcrysgr

Characterization of bulk hexagonal boron nitride single crystals grown by the metal flux technique



J.H. Edgar^{a,*}, T.B. Hoffman^a, B. Clubine^a, M. Currie^b, X.Z. Du^c, J.Y. Lin^c, H.X. Jiang^c

^a Kansas State University, Department of Chemical Engineering, Kansas State University, Manhattan, KS 66506, USA

^b Optical Sciences Division, Naval Research Laboratory, Washington, DC 20375, USA

^c Texas Tech University, Department of Electrical and Computer Engineering, Lubbock, TX 79409, USA

ARTICLE INFO

Available online 9 June 2014

Keywords:

A1. Optical absorption
B2. Photoluminescence
Hexagonal boron nitride
hBN
Single crystals

ABSTRACT

The optical and physical properties of hexagonal boron nitride single crystals grown from a molten metal solution are reported. The hBN crystals were grown by precipitation from a nickel–chromium flux with a boron nitride source, by slowly cooling from 1500 °C at 2–4 °C/h under a nitrogen flow at atmospheric pressure. The hBN crystals formed on the surface of the flux with an apparent crystal size up to 1–2 mm in diameter. Individual grains were as large as 100–200 μm across. Typically, the flakes removed from the metal were 6–20 μm thick. Optical absorption measurements suggest a bandgap of 5.8 eV by neglecting the binding energy of excitons in hBN. The highest energy photoluminescence peak was at 5.75 eV at room temperature. The hBN crystals typically had a pit density of $5 \times 10^6 \text{ cm}^{-2}$ after etching in a molten eutectic mixture of potassium hydroxide and sodium hydroxide. The quality of these crystals suggests they are suitable as substrates for two dimensional materials such as graphene and gallium nitride based devices.

© 2014 Elsevier B.V. All rights reserved.

1. Introduction

Single crystal hexagonal boron nitride (hBN) is the best substrate for supporting graphene, because of its similar crystal structure and lattice constants, ultrasmooth surfaces, low density of surface charge states, and wide energy band gap [1,2]. When it is encapsulated in hBN, graphene's properties are the best, including the highest reported room temperature charge carrier mobility ($> 140,000 \text{ cm}^2/\text{V s}$) [3] and ballistic transport distances of several microns [2,3].

hBN is also attractive as a substrate for other materials as well. Chan et al. [4] reported a ten-fold increase in the electron mobility of thin MoS₂ layers on hBN compared to SiO₂ substrates. Similarly, Gehring et al. [5] saw the surface carrier mobility of the topological insulator BiTe₂Se increase by a factor of three on hBN compared to SiO₂. hBN has also been proposed as a substrate for atomically thin layers of silicon (silicene) [6] and germanium (germanene) [7]. Since hBN does not have dangling surface bonds, the epitaxial layers it supports are weakly held and can be mechanically removed, allowing their separation from the substrate, as has been demonstrated for GaN based devices by Makimoto et al. [8] and Kobayashi et al. [9].

For all of these applications, single crystals are preferable to polycrystals because the properties of the layer changes with their relative crystallographic orientation to the hBN. That is, grain boundaries can disturb the electrical properties. Ideally, the hBN single crystals should have low defect densities, as these can also adversely affect the layers it supports. Furthermore, high purity hBN crystals are best, to ensure maximum optical transparency over a large range of wavelengths. Thus, this study was undertaken to determine the properties of hBN single crystals that were produced by the flux growth.

There have been relatively few studies on the bulk crystal growth of hBN [10–14]. These employed a variety of solvents for hBN including silicon [10], copper [11], sodium [12], and nickel–chromium [13,14]. Here we adapt the method developed by Kubota et al. [14] employing a Ni–Cr flux, due to its relatively modest temperature, ability to achieve reasonably fast growth rates, and ability to produce crystals at atmospheric pressure.

2. Experimental

For these studies, the hBN single crystals were precipitated from a 49 wt% nickel–51 wt% chromium flux that was used to dissolve the hBN powder source. The mixture was heated to 1500 °C under a flow of nitrogen at atmospheric pressure, and then slowly cooled at 4 °C/h to 1250 °C. A more complete

* Corresponding author.

E-mail address: edgarjh@ksu.edu (J.H. Edgar).

description of the crystal growth process was given in our earlier publication [15]. At room temperature, hBN flakes were mechanically peeled off of the solidified metal flux for further study.

Using micro-positioners, a h-BN flake was positioned over a 200- μm open aperture in a Au coated surface. Optical images of this structure are shown in Fig. 1. Optical transmission data through the flake and 200- μm pinhole were measured over a range from 1 to 6 eV using a Cary 5G spectrophotometer in dual-beam mode. The system baseline was calibrated using an identical 200- μm aperture without the BN flake.

For PL measurements, a frequency-quadrupled Ti-sapphire laser (with photon wavelength of 197 nm, 76 MHz repetition rate, and 100 fs pulse width) was used as an excitation source. The laser beam was focused onto the sample surface with a lens. The PL signal was collected and dispersed by a monochromator (1.3 m), and then detected by a microchannel-plate photo-multiplier tube together with a single photon-counting system [16].

To assess their quality, several hBN crystals were etched in a molten eutectic mixture of sodium hydroxide and potassium hydroxide at 430 °C for 1.5 min. Etch pits were assumed to be associated with dislocations in the crystals, as has been shown for other materials in this defect sensitive etchant [17]. Etch pit shapes, sizes, and densities were determined by scanning electron microscopy.

3. Results

The individual crystals nucleated with their (0001) planes parallel to the metal surface, but with random in-plane orientations. The hBN crystals that formed had an apparent size as indicated by their distinctive boundaries of up to 1–2 mm. Closer inspections showed that the individual grain size was up to 100–200 μm across. The thickness of the crystals ranged between 6 and 20 μm , as measured by surface profilometry. Frequently, the crystals were cracked, presumably due to contraction as the metal flux solidified, and the differences in the coefficients of thermal expansion of the hBN and the metal flux.

The measured optical transmission spectrum for a h-BN flake is shown in Fig. 2. To determine the BN thickness, the oscillations near 2 eV were fit to a Fabry–Perot cavity formed by the BN flake. Using 1.85 for the refractive index of BN [18], this provides an estimated thickness of 6.1 μm (see Fig. 2b). Knowing the thickness allows us to calculate the spectral absorption coefficient of this h-BN flake, as shown in Fig. 3.

The absorption coefficient is related to the bandgap (to first order) by $\alpha \propto (\hbar\omega - E_g)^n$,

where n is $\frac{1}{2}$ and 2 for direct and indirect bandgap materials, respectively. The spectral data are plotted in Fig. 4 as a function of (a) α^2 and (b) $\alpha^{1/2}$ to help identify the band-structure. The quality of linear fit to the data suggests an indirect gap of 5.8 eV. However, the rather wide bandgap of BN causes Coulomb attraction of e–h pairs as well as other effects that may influence the shape of h-BN's bandedge.

The maximum room temperature photoluminescence peak energy for the hBN flake (Fig. 5) was at 5.75 eV, which is similar to that reported for the best quality hBN single crystals [19]. Additional peaks were seen at 5.57 eV, which Watanabe et al. [20] attribute to stacking disorder, and at 4.45 eV, which is possibly associated with impurities.

Etching produced two types of hexagonal pits: those with pyramidal sidewalls converging to a point at the bottom of the pit, and those with a flat surface at the bottom of the pit (Fig. 6a). The flat bottom pits may indicate that the dislocation came to an end on the flat plane, or its path moved horizontal, in the plane. The etch pit density was typically $5 \times 10^6 \text{ cm}^{-2}$ in the broad areas

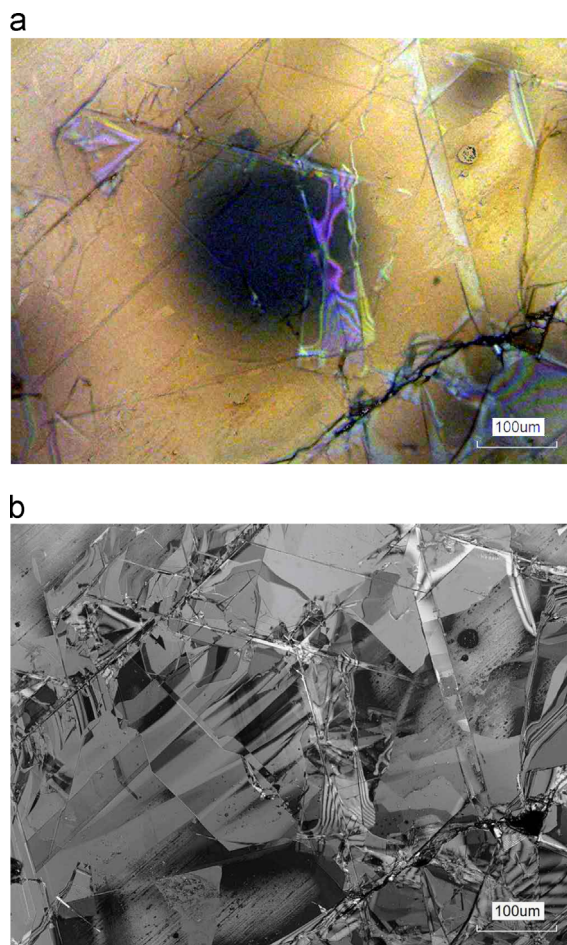


Fig. 1. Confocal microscope images of the h-BN flake mounted on a 200- μm aperture in a Au coated surface using (a) white light, and (b) 400-nm laser light.

of the individual grains. Not unexpectedly, the etch pit densities were higher at grain boundaries.

4. Discussion

The measurements made in this study demonstrate that the hBN produced by the flux method are of excellent structural and optical quality. The method is relative simple, requiring neither an excessive temperature nor pressure, suggesting the technique can be scaled to produce large crystals. It can produce hBN crystals that are relatively thick in comparison hBN prepared by thin film techniques.

Whether hBN has a direct or indirect bandgap has been debated in the literature. From ab initio calculations, Blase et al. [21] predicted that bulk hBN has an indirect band gap of 5.4 eV. On the basis of ultraviolet luminescence at 5.765 eV at room temperature and intrinsic fundamental absorption spectra with peaks between 5.822 eV and 5.968 eV at low temperature (8 K) with an s-like exciton structure, Watanabe et al. [19] claimed its bandgap is direct. Based on the intense photoluminescence at low temperature from epitaxial hBN layers deposited on sapphire substrates, Majety et al. [16] also supported the finding that hBN is a direct bandgap semiconductor. Using state-of-the art all-electron GW approximation, Arnaud et al. [22] asserted hBN is in fact an indirect band gap semiconductor. They estimated the minimum indirect and direct gaps as 5.95 eV and 6.47 eV respectively. The absorption measurement results shown in Fig. 4 seem to suggest that hBN has an indirect bandgap.

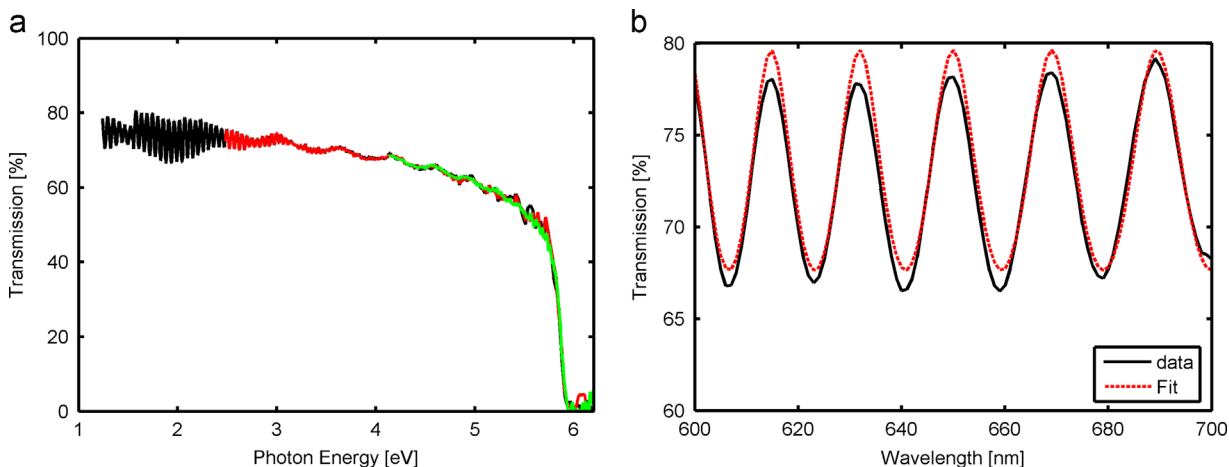


Fig. 2. a) Optical transmission spectrum of a h-BN flake from 1 to 6 eV, along with (b) a fit to the Fabry–Perot oscillations providing an 6.1- μm estimated thickness.

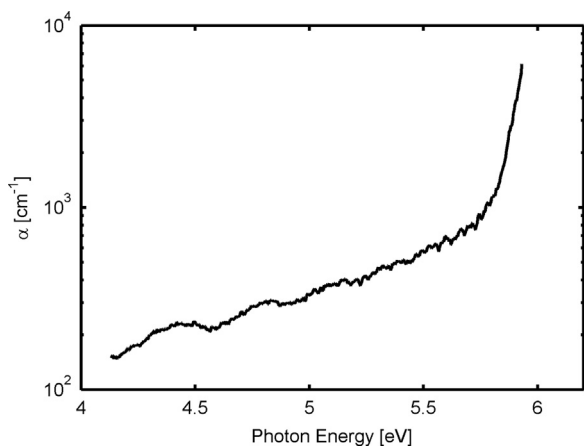


Fig. 3. Absorption coefficient for 6.1- μm thick h-BN flake.

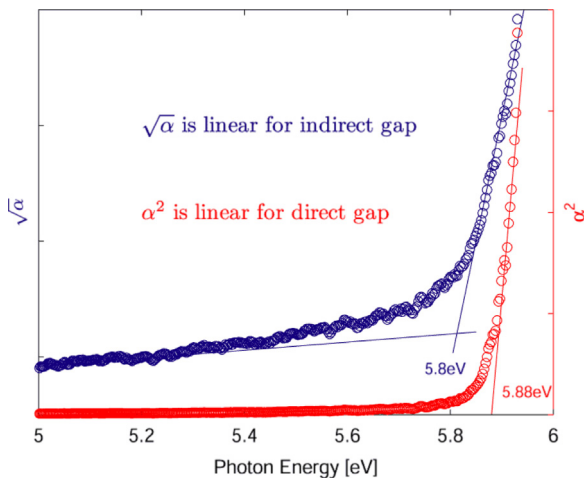


Fig. 4. Linear fit to spectral data assuming proportionality to α^2 and $\alpha^{1/2}$ to estimate the type of bandgap for the h-BN flake.

Liu et al. [23] and Gao [24] both predict that variations in the stacking sequence of layers modify the band gap magnitude and whether it is direct or indirect. Specifically, Liu et al. [23] writes there exists a substable structure of hBN, which corresponds to a glide distance of B–N bond length (1.446 Å) of all B layers of an ABAB... stacking aligning in a direction of in-plane B–N bond that is indirect. This configuration is quite stable and its total energy is only slightly above the ground state and forms a direct band with

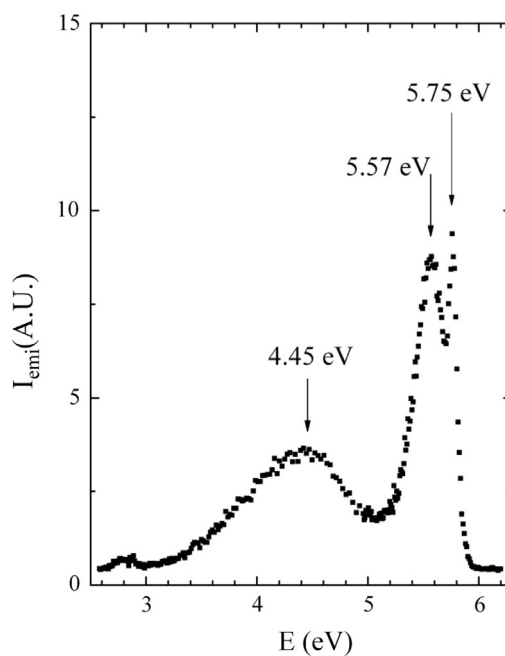


Fig. 5. Room temperature photoluminescence from a hBN crystal.

an energy gap of about 0.6 eV smaller than that of the ground state. Perhaps the structure of layer stacking of hBN may be different for materials grown by different methods, which could contribute to the debate regarding whether hBN has a direct or indirect bandgap. Our experimental results support a gap of 5.8 eV. Measured absorption at energies below the gap up to 5.5 eV show an exponential fit with energy suggesting Urbach tail states due to the disorder (polycrystallinity, etc.). The transition region between Urbach tail states and the indirect band edge could include states from dangling bonds, similar to those found in micro- and polycrystalline Si films. However, despite the debating issue concerning the bandgap, clearly, the band-edge emission efficiency in hBN is unusually high due to its layered structure [25]. The layer structured hBN provides a natural 2D system which result in a sharp “step”-like density of states and increase in the exciton binding energy and oscillator strength.

For the bulk hBN crystals, the grain size is larger and their defect densities are much lower than those typically found in the deposited thin films. For example, for their thin films, Tay et al. [26] reported a typical hBN domain size that was less than 1.0 square microns. Using transmission electron microscopy,

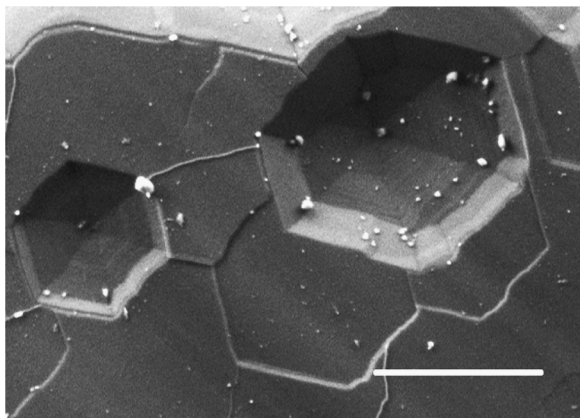


Fig. 6. Scanning electron microscope image of an individual pit formed by etching an hBN crystal in a eutectic mixture of potassium hydroxide and sodium hydroxide. The hexagonal pits had either pointed or flat bottoms (scale bar = 4.0 μm).

Levendorf et al. [27] established their hBN grain size was on the order of 1–10 μm . Lee et al. [28] observed the domain size of their hBN layers were determined by the grain size of the nickel foil they employed, on the order of 100 microns or less. For the hBN samples grown in this study, the grain size regularly exceeded 100 μm , and the potential exist for increasing the size further by modifying and improving the process.

5. Conclusions

Hexagonal boron nitride single crystals of good quality were produced from a nickel–chromium molten metal flux at atmospheric pressure. Optical absorption, photoluminescence, and defect selective etching demonstrates hBN's wide energy bandgap (5.8 eV), high energy peak (5.76 eV), and relatively low etch pit densities respectively. Additional studies are needed to eliminate cracking, increasing the crystal size, identifying the impurities present, and to further reduce the defect densities. With these improvements, this process may produce large area hBN crystals.

Acknowledgments

Funding for this project was made possible thanks to the National Science Foundation and U.S. Department of Homeland Security through funding of the Academic Research Initiative (ARI) program, ARI-MA Grant number 1038890, and a gift from the II–VI Foundation. M.C. acknowledges support from the Office of Naval Research.

References

- [1] C.R. Dean, A.F. Young, I. Meric, C. Lee, L. Wang, S. Sorgenfrei, K. Watanabe, T. Taniguchi, P. Kim, K.L. Shepard, J. Hone, Boron nitride substrates for high-quality graphene electronics, *Nat. Nanotechnol.* 5 (2010) 722–726.
- [2] A.S. Mayorov, R.V. Gorbachev, S.V. Morozov, L. Britnell, R. Jalil, L. A. Ponomarenko, P. Blake, K.S. Novoselov, K. Watanabe, T. Taniguchi, A. K. Geim, Micrometer-scale ballistic transport in encapsulated graphene at room temperature, *Nano Lett.* 11 (2011) 2396–2399.

- [3] L. Wang, I. Meric, P.Y. Huang, Q. Gao, Y. Gao, H. Tran, T. Taniguchi, K. Watanabe, L.M. Campos, D.A. Muller, J. Guo, P. Kim, J. Hone, K.L. Shepard, C.R. Dean, One-dimensional electrical contact to a two-dimensional material, *Science* 343 (2013) 614–617.
- [4] M.Y. Chan, K. Komatsu, S.-L. Li, Y. Xu, P. Darmawan, H. Kuramochi, S. Nakaharai, A. Aparecido-Ferreira, K. Watanabe, T. Taniguchi, K. Tsukagoshi, Suppression of thermally activated carrier transport in atomically thin MoS_2 on crystalline hexagonal boron nitride substrates, *Nanoscale* 5 (2013) 9572–9576.
- [5] P. Gehring, B.F. Gao, M. Burghard, K. Kern, Growth of high-mobility BiTe_2Se nanoplatelets on hBN sheets by van der Waals epitaxy, *Nano Lett.* 12 (2012) 5137–5142.
- [6] L. Li, X. Wang, X. Zhao, M. Zhao, Moiré superstructures of silicene on hexagonal boron nitride: a first-principles study, *Phys. Lett. A* 377 (2013) 2628–2632.
- [7] L. Li, M. Zhao, First-principles identifications of superstructures of germanene on $\text{Ag}(111)$ surface and h-BN substrate, *Phys. Chem. Chem. Phys.* 15 (2013) 16853.
- [8] T. Makimoto, K. Kumakura, Y. Kobayashi, T. Akasaka, H. Yamamoto, A vertical InGaN/GaN light-emitting diode fabricated on a flexible substrate by a mechanical transfer method using BN, *Appl. Phys. Express* 5 (2012) 072102.
- [9] Y. Kobayashi, K. Kumakura, T. Akasaka, T. Makimoto, Layered boron nitride as a release layer for mechanical transfer of GaN-based devices, *Nature* 484 (2012) 223–227.
- [10] T. Ishii, T. Sato, Growth of single crystals of hexagonal boron nitride, *J. Cryst. Growth* 61 (1983) 689–690.
- [11] M. Hubáček, T. Sató, The effect of copper on the crystallization of hexagonal boron nitride, *J. Mater. Sci.* 32 (1997) 3293–3297.
- [12] M. Yano, M. Okamoto, Y.K. Yap, M. Yoshimura, Y. Mori, T. Sasaki, Growth of nitride crystals BN, AlN and GaN by using a Na flux, *Diam. Relat. Mater.* (2000) 512–515.
- [13] Y. Kubota, K. Watanabe, O. Tsuda, T. Taniguchi, Deep ultraviolet light-emitting hexagonal boron nitride synthesized at atmospheric pressure, *Science* 317 (2007) 932–934.
- [14] Y. Kubota, K. Watanabe, O. Tsuda, T. Taniguchi, Hexagonal boron nitride single crystal growth at atmospheric pressure using Ni–Cr solvent, *Chem. Mater.* 20 (2008) 1661–1663.
- [15] T.B. Hoffman, B. Clubine, T. Zhang, K. Snow, J.H. Edgar, Optimization of Ni–Cr flux growth for hexagonal boron nitride single crystals, *J. Cryst. Growth* 393 (2014) 114–118, <http://dx.doi.org/10.1016/j.jcrysgro.2013.09.030>.
- [16] S. Majety, X.K. Cao, J. Li, R. Dahal, J.Y. Lin, H.X. Jiang, Band-edge transitions in hexagonal boron nitride epilayers, *Appl. Phys. Lett.* 101 (2012) 051110.
- [17] J.L. Weyher, Defect sensitive etching of nitrides: appraisal of methods, *Cryst. Res. Technol.* 47 (2012) 333–340.
- [18] O. Stenzel, J. Hahn, M. Roeder, A. Ehrlich, S. Prause, F. Richter, The optical constants of cubic and hexagonal boron nitride thin films and their relation to the bulk optical constants, *Phys. State Solidi A* 158 (1996) 281–287.
- [19] K. Watanabe, T. Taniguchi, H. Kanda, Direct-bandgap properties and evidence for ultraviolet lasing of hexagonal boron nitride single crystal, *Nat. Mater.* 3 (2004) 404–409.
- [20] K. Watanabe, T. Taniguchi, T. Kuroda, H. Kanda, Effects of deformation on band-edge luminescence of hexagonal boron nitride single crystals, *Appl. Phys. Lett.* 89 (2006) 141902.
- [21] X. Blase, A. Rubio, S.G. Louie, M.L. Cohen, Quasi-particle band structure of bulk hexagonal boron-nitride and related systems, *Phys. Rev. B* 51 (1995) 6868–6875.
- [22] B. Arnaud, S. Lebegue, P. Rabiller, M. Alouani, Huge excitonic effects in hexagonal boron nitride, *Phys. Rev. Lett.* 96 (2006) 026402.
- [23] L. Liu, Y.P. Feng, Z.X. Shen, Structure and electronic properties of h-BN, *Phys. Rev. B* 68 (2003) 104102.
- [24] S.-P. Gao, Crystal structures and band gap characters of h-BN polytypes predicted by the dispersion corrected DFT and GW methods, *Solid State Commun.* 152 (2012) 1817–1820.
- [25] B. Huang, X.K. Cao, H.X. Jiang, J.Y. Lin, S.H. Wei, Origin of the significantly enhanced optical transitions in layered boron nitride, *Phys. Rev. B* 86 (2012) 155202.
- [26] R.Y. Tay, X. Wang, S.H. Tsang, G.C. Loh, R.S. Singh, H. Li, G. Mallick, E.H.T. Teo, A systematic study of the atmospheric pressure growth of large-area hexagonal crystalline boron nitride film, *J. Mater. Chem. C* 2 (2014) 1650–1657.
- [27] M.P. Levendorf, C.-J. Kim, L. Brown, P.Y. Huang, R.W. Havener, D.A. Muller, J. Park, Graphene and boron nitride lateral heterostructures for atomically thin circuitry, *Nature* 488 (2012) 627–632.
- [28] Y.-H. Lee, K.-K. Liu, A.-Y. Lu, C.-Y. Wu, C.-T. Lin, W. Zhang, C.-Y. Su, C.-L. Hsu, T.-W. Lin, K.-H. Wei, Y. Shi, L.-J. Li, Growth selectivity of hexagonal-boron nitride layers on Ni with various crystal orientations, *RSC Adv.* 2 (2012) 111–115.